

Article ID: 1001-0742(2002)04-0433-06

CLC number: X13

Document code: A

Numerical simulation of the sedimentation of cylindrical pollutant particles in fluid

LIN Jian-zhong¹, WANG Ye-long¹, WANG Wei-xiong¹, YU Zhao-sheng²

(1. Department of Mechanics, Zhejiang University, Hangzhou 310027, China. E-mail: meejzlin@public.zju.edu.cn; 2. Department of Mechanical and Mechatronic Engineering, the University of Sydney, NSW 2006, Australia)

Abstract: The sedimentation of cylindrical pollutant particles which fall through a fluid is investigated. Differing from previous research work, particle oscillation and effect of particle on the fluid are considered, and the torque exerted on a particle when viscous fluid flow around a particle is got through experiment and included in the numerical simulation. The computational results showed that the sedimentation velocities of particle increase slowly with the increase of particle aspect ratio ϕ . For disk-like particle, when the motion direction of particle is parallel to axis of particle, particle falls more slowly than the case of perpendicular to axis of particle; while for rod-like particle, it is inverse. For sedimentation of a crowd of high-frequency oscillating cylindrical particles with arbitrary initial orientation, both vertical velocity and horizontal velocity oscillate dramatically, the degree of oscillation of the former is stronger than the later. A crowd of particles fall more quickly than an isolated particle. Particles tend to strongly align in the direction of gravity. The computational results agreed well with the experimental ones and helpful for controlling of pollutant particles.

Keywords: cylindrical pollutant particles; sedimentation; orientation; velocity; numerical simulation

Introduction

What pollutant particles suspend in air or water is one of the main environmental pollution. Usually the pollutant particles move in the form of sedimentation. The restraint of environmental pollution can be achieved by controlling the sedimentation of pollutant particles. Therefore, it is important to comprehend the laws of sedimentation of particles. And sedimentation of particles is also one of the most basic kinds of motion of fluid-particle suspension and is the basis of some laboratory techniques for determining the distribution of particles sizes in a particulate dispersion.

The sedimentation of particles has been extensively studied. However, there is less known about the sedimentation of cylindrical particle, as a matter of fact, a lot of pollutant particles are cylindrical. Koch and Shaqfeh (Koch, 1989) considered the sedimentation of axisymmetric, nonspherical particles in dilute suspension including only two body interparticle interactions and demonstrated that due to the coupling between center-of-mass and orientation motion, particle "clumping" or "streaming" should occur. Turney *et al.* (Turney, 1995) examined the sedimentation of polymethyl methacrylate rods using NMR imaging and presented the hindered settling function for a range of volume loadings. Herzhaft *et al.* (Herzhaft, 1996) measured the mean sedimentation velocity, variance of the sedimentation velocity, and the orientation distribution and found a steady state where the cylindrical particles "clump" together and tend to align in the direction of gravity with occasional "flipping". Mackaplow *et al.* (Mackaplow, 1998) studied the sedimentation of particle suspension at low Reynolds number using both Monte Carlo and dynamic simulations. For homogeneous, isotropic suspensions, the Monte Carlo simulations show that the hindrance of the mean sedimentation speed is linear in particle concentration up to some extent. The dynamic simulations, however, show that interparticle hydrodynamic interactions cause the spatial and orientational distributions to become inhomogeneous and anisotropic. Most of the particles migrate into narrow streamers aligned in the direction of gravity. Up to now, there are no numerical results about sedimentation of cylindrical particles with consideration of particle oscillation, the torque caused when viscous fluid flow around cylindrical particle. Actually, in the case of low Reynolds number, the sedimentation of cylindrical

particles is always accompanied with the oscillation, and the torque caused when viscous fluid flow around cylindrical particle plays a key role for the rotation of particles.

It is the purpose of the present work to report on numerical results, under the consideration of above factors, which show the effect of particle aspect ratio on the mean sedimentation velocity, the motion of particles with arbitrary initial orientation.

1 Numerical model

1.1 Force acting on a cylindrical particle

Fig.1 shows cylindrical particle and two cases of sedimentation. In the paper, we restrict ourselves to suspensions meeting the conditions that both the particle and fluid Reynolds numbers are much less than unity, so inertia can be neglected. The force acting on a cylindrical particle consists of three parts:

The first part is the net gravity of particle in fluid. It equals to the difference of gravity and buoyancy acting on the particle:

$$F_1 = (\rho_p - \rho_f) V_p g = 2\pi\phi(\rho_p - \rho_f) a^3 g, \quad (1)$$

where V_p is the volume of particle, ϕ is the particle aspect ratio, a is the radius of particle.

The second part is hydrodynamic force on a cylindrical particle with high-frequency oscillating (Pozrikidis, 1989):

$$F_2 = \mu a Re \left\{ A^{-1} \left[\beta D + \lambda B^\infty + \lambda^2 M^A + \frac{\lambda}{\lambda + 1} \left(\frac{1}{6\pi} D \cdot D - B^\infty \right) \right] A \cdot U_0 e^{-i\omega t} \right\}, \quad (2)$$

where the μ is the viscosity, Re is to get the real part, A is a transformation matrix, $A = \begin{bmatrix} \cos\theta & \sin\theta \\ -\sin\theta & \cos\theta \end{bmatrix}$, θ is the angle of particle's axis to x axis of Cartesian coordinates. β is a parameter reflecting the interaction among particles, and is taken to be about 2/3 according to the experimental results (Hertzhaft, 1996). D is the frictional resistance tensor for steady Stokes flow, B^∞ is the Basset force, λ is a frequency factor, $\lambda^2 = -i\omega a^2/\nu$, ω is the oscillating frequency, ν is the viscosity, M^A is the added mass force, U_0 is the random oscillating velocity. Here $|\lambda| = O(1)$, so $\omega = O\left(\frac{\nu}{a^2}\right)$, then we can simplify Eq.(2) into:

$$F_2 = c_1 \beta \cos\omega t A^{-1} D A \cdot U_0 + c_2 (\cos\omega t - \sin\omega t) A^{-1} B^\infty A \cdot U_0 + c_3 \sin\omega t A^{-1} M^A A \cdot U_0 + c_4 [(2k + 1)\cos\omega t - \sin\omega t] A^{-1} \left(\frac{1}{6\pi} D \cdot D - B^\infty \right) A \cdot U_0, \quad (3)$$

where $c_1 = -\mu a$, $c_2 = -k\mu a$, $c_3 = 2k^2\mu a$, $c_4 = -\frac{k}{2k^2 + 2k + 1} \cdot \mu a$, $k = a\sqrt{\frac{\omega}{2\nu}}$.

The third part is the Stokes resistance, it can be expressed as:

$$F_3 = -\mu a \beta A^{-1} D A \cdot (U - U_0), \quad (4)$$

where U_0 is the particle velocity, U is the fluid velocity at center of particle. When a crowd of particles are simulated, the U in different positions are different because of the wake of particles, which can be expressed as Eq.(5) approximately based on Fig.2 (White, 1974).

$$U = U_0 - u = U_0 - C \frac{1}{\sqrt{x}} \exp\left(-\frac{U_0 y^2}{4\nu x}\right), \quad (5)$$

where C is 1.76, then force acting on a cylindrical particle is:

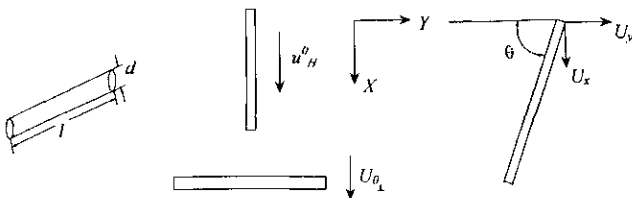


Fig.1 Sketch map of sedimentation of cylindrical particle

$$F = F_1 + F_2 + F_3. \tag{6}$$

1.2 Torque acting on a cylindrical particle

The torque acting on a cylindrical particle has two parts, the first part is the resistant torque caused by rotation of particle (Cox, 1970):

$$T_1 = -\frac{1}{3}\pi\mu\sigma l^3 d[1 - \sigma(\ln 2 - 1.8333)]\dot{\theta}, \tag{7}$$

where $\sigma = \ln^{-1}(2\phi)$, d is the diameter of particle.

The second part, T_2 , is the torque caused when viscous fluid flow around cylindrical particle. T_2 changes with the orientation of particle and always tries to cause the particle to turn back to a steady orientation. When the Reynolds number is large, T_2 will be much smaller than T_1 . In the case of sedimentation, T_1 and T_2 have similar quantities, so we must consider T_1 and T_2 simultaneously. There is not ready equation for T_2 till now. In order to get the expression of T_2 , we measure the T_2 in a wind tunnel as shown in Fig.3. Fig.4 shows the relationship between T_2 and θ with different particle aspect ratio ϕ .

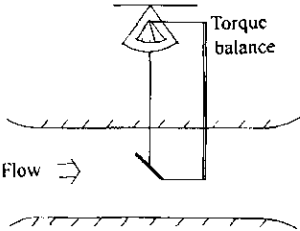


Fig.3 Experimental facility

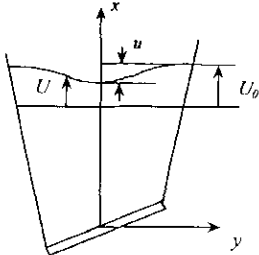


Fig.2 Wake of cylindrical particle

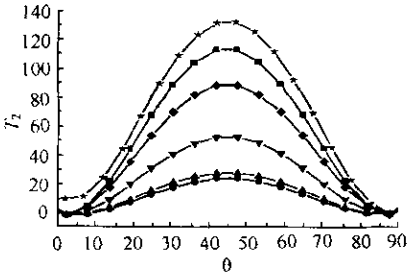


Fig.4 Relationship between T and θ

● : $\phi = 10.6$; ▲ : $\phi = 20$; ▼ : $\phi = 25$;
◆ : $\phi = 30$; ■ : $\phi = 35$; ★ : $\phi = 40$

Fitting the curves in Fig.4 with 3-order polynomial, we have expressions of T_2 for different ϕ :

$$T_2 = F(\theta, \theta^2, \theta^3, \phi, \alpha), \tag{8}$$

where α is a constant.

Then torque acting on a cylindrical particle is:

$$T = T_1 + T_2. \tag{9}$$

1.3 Motion equation and rotation equation for particle

Motion equation of cylindrical particle is:

$$\begin{bmatrix} \ddot{x} \\ \ddot{y} \end{bmatrix} = \frac{F_1 + F_2 + F_3}{m_p} = \frac{\rho_p - \rho_f}{\rho_p} \begin{bmatrix} g \\ 0 \end{bmatrix} + \begin{bmatrix} a_1 & a_2 \\ a_3 & a_4 \end{bmatrix} \begin{bmatrix} U_{0x} \\ U_{0y} \end{bmatrix} + \begin{bmatrix} b_1 & b_2 \\ b_3 & b_4 \end{bmatrix} \begin{bmatrix} \dot{x} - U_{0x} \\ \dot{y} - U_{0y} \end{bmatrix}, \tag{10}$$

where a_i and b_i stand for related terms in Eqs. (1), (3) and (4).

Rotation equation of particle is:

$$\ddot{\theta} = \frac{1}{J_p} (T_1 + T_2), \tag{11}$$

where

$$J_p = \frac{m_p}{12} (6a^2 + l^2), \tag{12}$$

here l is the length of particle.

2 Results and discussion

Before calculating Eq. (10), the B^* and M^A should be determined. Here B^* and M^A are obtained by fitting the curves given from experimental results (Loewenberg, 1993) with 6-order polynomial. The expressions are:

$$B_{\parallel}^* = 15.96 + 13.81\phi - 55.52\phi^2 + 166.46\phi^3 - 241.47\phi^4 + 167.32\phi^5 - 43.97\phi^6, 0.01 \leq \phi \leq 1$$

$$B_{\parallel}^* = 18.98 - 2.79\phi + 0.20\phi^2 - 0.01\phi^3, 1 \leq \phi \leq 100$$

$$B_{\perp}^* = 11.35 + 10.89\phi + 44.31\phi^2 - 94.74\phi^3 - 179.69\phi^4 + 480.89\phi^5 - 254.63\phi^6, 0.01 \leq \phi \leq 1$$

$$B_{\perp}^* = 20.46 - 2.64\phi + 0.19\phi^2 - 0.01\phi^3, 1 \leq \phi \leq 100$$

$$M_{\parallel}^A = 2.58 + 10.19\phi - 71.27\phi^2 + 258.37\phi^3 - 470.03\phi^4 + 411.06\phi^5 - 137.2\phi^6, 0.01 \leq \phi \leq 1$$

$$M_{\parallel}^A = 3.58 + 0.10\phi - 0.001\phi^2, 1 \leq \phi \leq 100$$

$$M_{\perp}^A = 4.58 - 21.65\phi + 138.45\phi^2 - 459.84\phi^3 + 783.35\phi^4 - 652.67\phi^5 + 210.25\phi^6, 0.01 \leq \phi \leq 1$$

$$M_{\perp}^A = 3.58 + 0.43\phi - 0.03\phi^2, 1 \leq \phi \leq 100$$

2.1 The sedimentation velocities of cylindrical particle

When a particle with initial orientation $\theta = \pi/2$ falls through a fluid. During the sedimentation, the particle keeps $\theta = \pi/2$. In this case, the sedimentation velocities are shown in Fig.5. For the case of $\theta = 0$, the results are shown in Fig.6. In the Fig.5 and 6, the curves are the experimental results (Heiss, 1952) and the solid round points represent calculated results in this paper. The calculated results agreed with experimental ones very well. From the figures, we can see that: (1) Both two cases of $\theta = 0$ and $\theta = \pi/2$, the sedimentation velocities of particle increase slowly with the increase of particle aspect ratio ϕ . (2) For disk-like particle ($\phi < 1$), the particle with $\theta = \pi/2$ falls more slowly than the case with $\theta = 0$; while for rod-like particle ($\phi > 1$) it is inverse. (3) For disk-like particle, sedimentation velocities for both cases of $\theta = \pi/2$ and $\theta = 0$ do not differ largely, and difference of velocities for two cases decreases with the increase of ϕ , however, for the rod-like particle, the difference will increase with the increase of ϕ .

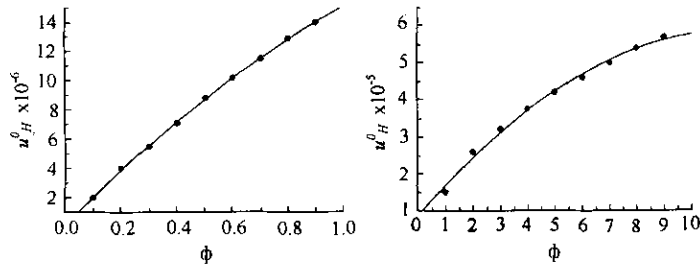


Fig.5 The sedimentation velocities of particle with $\theta = \pi/2$

—: experimental results; ●: calculated results

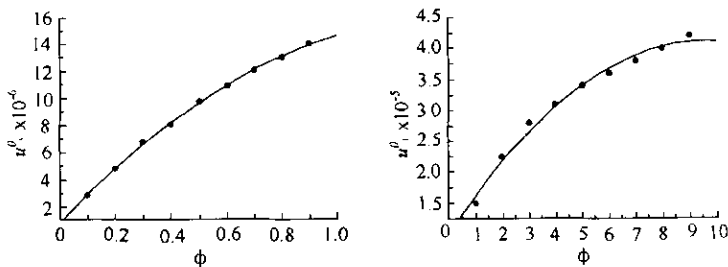


Fig.6 The sedimentation velocities of particle with $\theta = 0$

—: experimental results; ●: calculated results

2.2 Sedimentation of high-frequency oscillating particles with arbitrary initial orientation

The calculation for two hundreds of high-frequency oscillating particles with arbitrary initial orientation is performed. Fig. 7 is the results of a typical particle versus time, (a) is the sedimentary velocity which is normalized relative to the maximum velocity that an isolated cylindrical particle can achieve, in which the upper is the vertical velocity u_x and the below is the horizontal velocity u_y , (b) is the orientation θ of particle versus time. Fig. 8 is the corresponding experimental results (Herzhaft, 1996). In order to determine whether a steady state can be reached, the mean vertical velocities, the mean horizontal velocities and the mean projected angles, ensemble averaged over two hundreds of particle trajectories are plotted versus time t in Fig. 9. Fig. 10 is the corresponding experimental results (Herzhaft, 1996), in which for each time, t , the number of instantaneous velocities of projected angles used in the statistical ensemble varied between 20 and 70. The calculated and the experimental results are the same roughly. It can be seen from the figures that:

(1) In Fig. 7a, both vertical velocity u_x and horizontal velocity u_y oscillate dramatically, the degree of oscillation of the former is stronger than the later. The vertical velocities are usually greater than 1, its mean value is about 1.5. This means that a crowd of particles fall more quickly than single particle. The values of horizontal velocity fluctuate around 0.

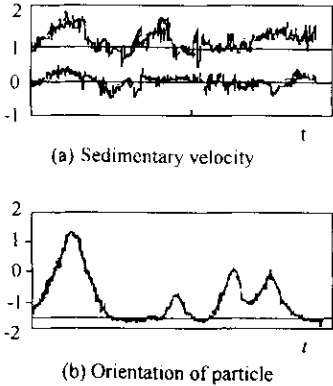


Fig.7 The calculated results for a typical particle

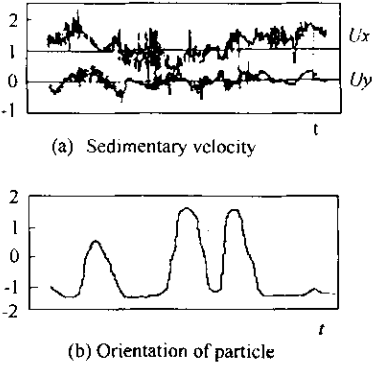


Fig. 8 The corresponding experimental results (Herzhaft, 1996)

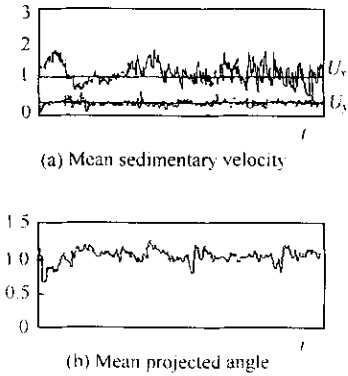


Fig.9 The mean values over two hundreds of particle trajectories with arbitrary initial orientation

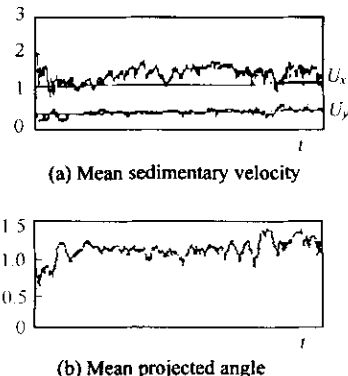


Fig.10 The corresponding experimental results (Herzhaft, 1996)

(2) In Fig. 7b, the orientation of typical particle changes versus time and tends to align in the vertical direction, this means the particles will range along gravity. During the change of orientation, there are fluctuations with very small amplitude because of high-frequency oscillating of particle, this

phenomenon is not observed in the experimental results (Fig. 8b).

(3) In Fig. 9, the velocities seem to reach a steady state after certain time, where (u_x) fluctuates around a value larger than 1 and (u_y) around zero. The mean projected angle also reaches a steady state after certain time, where it fluctuates around a value about 1.2 rad which corresponds to particles perfectly aligned in the vertical direction.

3 Conclusions

The method put forward in this paper can perfectly predict the sedimentation of cylindrical particle in fluid.

When a single particle falls through a fluid with a constant orientation, the sedimentation velocities of particle increase slowly with the increase of particle aspect ratio ϕ . For disk-like particle, the particle with $\theta = \pi/2$ falls more slowly than the case with $\theta = 0$; while for rod-like particle, it is inverse. For disk-like particle, the sedimentation velocities for both cases of $\theta = \pi/2$ and $\theta = 0$ do not differ largely, and difference of velocities for two cases decreases with the increase of ϕ . However, for the rod-like particle, the difference will increase with the increase of ϕ .

For the sedimentation of a crowd of high-frequency oscillating particles with arbitrary initial orientation, both vertical velocity and horizontal velocity oscillate dramatically, the degree of oscillation of the former is stronger than the later. The vertical mean sedimentation velocities for a crowd of particles are larger than an isolated vertical particle. The particles tend to strongly align in the direction of gravity.

References:

- Cox R G, 1970. Long slender bodies in a viscous fluid [J]. *J Fluid Mech*, 44: 792—821.
- Heiss J F, Coull J, 1952. The effect of orientation and shape on the settling velocity of non-isometric particles in a viscous medium[J]. *Chem Eng Prog*, 48:133—140.
- Herzhaft B, Guazzelli E, Michael B M *et al.*, 1996. Experimental investigation of the sedimentation of a dilute fiber suspension[J]. *Phys Review Letters*, 77: 290—293.
- Koch D L, Shaqfeh E S G, 1989. The instability of suspension of sedimenting spheroids[J]. *J Fluid Mech*, 209: 521—542.
- Loewenberg M, 1993. Stokes resistance, added mass, and Basset force for arbitrarily oriented, finite-length cylinders[J]. *Phys Fluids*, 5: 765—767.
- Mackaplow M B, Shaqfeh E S G, 1998. A numerical study of the sedimentation of fiber suspensions[J]. *J Fluid Mech*, 376: 149—182.
- Pozrikidis C, 1989. A singularity method for unsteady linearized flow[J]. *Phys Fluids*, A1(9): 1508—1512.
- Turney M A, Cheung M K, McCarthy M *et al.*, 1995. Hindered settling of rod-like particles measured with magnetic resonance imaging[J]. *AIChE J*, 41: 251—257.
- White F M, 1974. *Viscous fluid flow*[M]. McGraw-Hill Book Company.

(Received for review September 11, 2001. Accepted October 24, 2001)